2017

Three-dimensional tissues using human pluripotent stem cell spheroids as biofabrication building blocks

Haishuang Lin
University of Nebraska - Lincoln, hlin9@unl.edu

Qiang Li
University of Nebraska-Lincoln, qli18@unl.edu

Yuguo Lei
University of Nebraska - Lincoln, ylei14@unl.edu

Three-dimensional tissues using human pluripotent stem cell spheroids as biofabrication building blocks

Biofabrication

OPEN ACCESS

RECEIVED
12 October 2016

REVISED
27 February 2017

ACCEPTED FOR PUBLICATION
13 March 2017

PUBLISHED
20 April 2017

PAPER

Three-dimensional tissues using human pluripotent stem cell spheroids as biofabrication building blocks

Haishuang Lin[1,5], **Qiang Li**[1,2,5] **and Yuguo Lei**[1,2,3,4]

[1] Department of Chemical and Biomolecular Engineering, University of Nebraska, Lincoln, Nebraska, United States of America
[2] Biomedical Engineering Program, University of Nebraska, Lincoln, Nebraska, United States of America
[3] Mary and Dick Holland Regenerative Medicine Program, University of Nebraska Medical Center, Omaha, Nebraska, United States of America
[4] Fred & Pamela Buffett Cancer Center, University of Nebraska Medical Center, Omaha, Nebraska, United States of America
[5] These authors contribute equally.

E-mail: ylei14@unl.edu

Keywords: human pluripotent stem cells, spheroids, tissue biofabrication, organ bioprinting

Abstract

A recently emerged approach for tissue engineering is to biofabricate tissues using cellular spheroids as building blocks. Human pluripotent stem cells (hPSCs), including human embryonic stem cells (hESCs) and induced pluripotent stem cells (iPSCs), can be cultured to generate large numbers of cells and can presumably be differentiated into all the cell types of the human body *in vitro*, thus are an ideal cell source for biofabrication. We previously developed a hydrogel-based cell culture system that can economically produce large numbers of hPSC spheroids. With hPSCs and this culture system, there are two potential methods to biofabricate a desired tissue. In Method 1, hPSC spheroids are first utilized to biofabricate an hPSC tissue that is subsequently differentiated into the desired tissue. In Method 2, hPSC spheroids are first converted into tissue spheroids in the hydrogel-based culture system and the tissue spheroids are then utilized to biofabricate the desired tissue. In this paper, we systematically measured the fusion rates of hPSC spheroids without and with differentiation toward cortical and midbrain dopaminergic neurons and found spheroids' fusion rates dropped sharply as differentiation progressed. We found Method 1 was appropriate for biofabricating neural tissues.

1. Introduction

Tissue engineering combines engineering principles and life science to repair, regenerate or restore the formats and functions of injured or dysfunctional tissues or organs [1–4]. In scaffold-based tissue engineering, a porous material is fabricated using biocompatible and/or biodegradable polymers [5, 6]. Living cells are then seeded onto the scaffold and the construct is cultured in a bioreactor *in vitro* to achieve the desired cell density, mechanical properties and/or functions before implantation. This classic approach has achieved many successes, but also has limitations [1, 5–11]. For instance, it is very challenging to generate vasculature; to achieve the organ-level cell density; and to precisely place specific cell types at the desired position in the construct. The mechanical properties of the scaffold and the products resulting from the scaffold degradation sometimes change the cell viability, proliferation, phenotype and physiology. In addition, due to the slow scaffold degradation and tissue morphogenesis, this approach is labor, time and reagent consuming.

A recently emerged approach for tissue engineering is to biofabricate tissues using cellular spheroids as building blocks [5, 6, 12]. Large numbers of human cells are first obtained and processed into multicellular spheroids, with a diameter of hundreds of micrometers, through methods including re-aggregation, microfluidics, hanging drop, micro-molds, spinner culture and rotating wall vessels [5, 6, 12, 13]. With the re-aggregation method, cells are centrifuged in a tube to form a pellet that is then cut into small fragments that are subsequently cultured to form spheroids. With the hanging drop method, small volumes of cell suspensions are placed on a lid that is subsequently inverted to form hanging drops. Cells in each hanging drop aggregate to form one spheroid. With the microfluidic and micro-mold methods, cells are

placed in micro-wells to form one spheroid per well. With the spinner culture and rotating wall vessel methods, large numbers of cells are cultured in suspension in the spinner flasks or rotating wall vessels to simultaneously generate many spheroids. Next, the cellular spheroids are dispensed into a desired geometry, using a bio-printer or a mold. Upon contact, neighboring spheroids fuse to form a cohesive tissue due to the cell-cell and cell-matrix interactions. Lastly, the fused tissue is cultured in a bioreactor to mature before implantation.

This scaffold-free approach has been investigated for biofabricating many types of human tissue [13]. However, there are some challenges to be resolved [13]. The first is to obtain large numbers of human cells for the biofabrication. It is known that isolating large numbers of primary cells from a patient is challenging and only very limited human cell types can be cultured *in vitro*. In addition, when cultured, primary human cells quickly change phenotype and lose proliferation capability. Assuming we have sufficient cells, the second challenge is to quickly and reproducibly bioprocess them into uniform spheroids. The aforementioned re-aggregation, microfluidics, hanging drop, and micro-molds lack the capability to produce spheroids in large scale [13]. And with spinner culture and rotating wall vessel methods, the size and characteristics of the produced spheroids are not uniform [14, 15]. In addition, the numbers of spheroids that can be produced per volume of culture is low, resulting in high production costs [14, 15]. The third challenge is that, after being placed in position, spheroids fuse slowly, which will negatively impact the subsequent tissue maturation [13].

We explored whether these challenges could be resolved using human pluripotent stem cells (hPSCs) as the starting cell source. hPSCs, including human embryonic stem cells (hESCs) [16] and induced pluripotent stem cells (iPSCs) [17], can be cultured *in vitro* over a long term to generate large numbers of cells, and they can presumably be differentiated into all the cell types of the human body [18]. For instance, hPSCs have been successfully differentiated into cortical neurons [19, 20], gamma-aminobutyric acid interneurons [21–23], midbrain dopaminergic neurons [24, 25], endothelial cells [26–28], mesenchymal stem cells [29, 30], cardiomyocytes [31–33], hepatocytes [34–36], beta cells [37, 38] and other human cell types in the past decade. Additionally, patient-specific iPSCs and their derivatives (i.e. cells differentiated from iPSCs) induce minimal or no immune rejection in the patient. These characteristics make hPSCs an ideal cell source for tissue biofabrication.

Conventionally, hPSCs are cultured in two-dimensional (2D) dishes or flasks. However, these 2D culture systems are considered unsuitable for economic large-scale cellular biomanufacturing due to their low yield, scalability, and reproducibility [39, 40]. In addition, cells produced in 2D cell culture systems need further bioprocessing to form spheroids. To overcome this challenge, we previously developed a simple, efficient, scalable, and current Good Manufacturing Practice (cGMP) compliant three-dimensional (3D) culture system for expanding and differentiating hPSCs to generate hPSC spheroids and tissue spheroids (e.g. neuron spheroids) [14, 15, 40]. The system utilizes a thermoreversible PNIPAAm-PEG hydrogel as scaffolds for culturing hPSCs. Single hPSCs are suspended in liquid PNIPAAm-PEG polymer solution at ~4 °C. Upon heating to 37 °C, the polymer solution gels to form an elastic matrix, resulting in single hPSCs encapsulated in the hydrogel matrix that grow into uniform hPSC spheroids within the hydrogel. With further culturing in a differentiation medium, these hPSC spheroids can be differentiated into tissue spheroids. This culture system enables us to economically produce large numbers of hPSC and tissue spheroids for tissue biofabrication.

With hPSCs and this culture system, there are two potential methods to biofabricate a desired tissue. In Method 1, hPSC spheroids are utilized to biofabricate an hPSC tissue that is subsequently cultured in a medium capable of differentiating the hPSC tissue into the desired tissue. The key for Method 1 to succeed includes: (1) hPSC spheroids can quickly fuse to form an hPSC tissue, and (2) hPSCs in the hPSC tissue can be differentiated into the desired tissue cells. In Method 2, hPSC spheroids are first converted into tissue spheroids in the PNIPAAm-PEG hydrogel culture system and the tissue spheroids are utilized to biofabricate the desired tissue. Since we have shown hPSC spheroids could be efficiently differentiated into tissue spheroids in the PNIPAAm-PEG hydrogel [15, 41, 42], the key for Method 2 to succeed is that tissue spheroids can quickly fuse to form a cohesive tissue. In this paper, we will use the biofabrication of 3D neural tissues as examples to explore these questions and to find out which method is more appropriate for tissue biofabrication using hPSCs as cell source.

2. Materials and methods

2.1. Culturing hPSCs in 2D

iPSCs (iPSCs reprogrammed from human mesenchymal stem cells) were obtained from George Q. Daley laboratory (Children's Hospital Boston, Boston) [43]. H9 hESCs were purchased from WiCell Research Institute. hPSCs (iPSCs and H9s) were maintained in a 6-well plate coated with Matrigel (BD Biosciences) in Essential 8^{TM} medium (E8, Invitrogen) [18]. Cells were passaged every 4 days with 0.5 mM EDTA (Invitrogen) and the medium was changed daily. Cells were routinely checked for the expression of pluripotency markers, Oct4 and Nanog, their capability to form teratomas in immunodeficient mice, their karyotypes and bacterial contaminations.

2.2. Biomanufacturing hPSC spheroids in PNIPAAm-PEG hydrogels

To transfer the culture from 2D to 3D PNIPAAm-PEG hydrogels, hPSCs maintained in Matrigel-coated 6-well plate were treated with Accutase (Life Technologies) at 37 °C for 5 min and dissociated into single cells [14, 15]. Dissociated cells were mixed with 10% PNIPAAm-PEG (Cosmo Bio, USA) solution dissolved in E8 medium on ice and cast on tissue culture plate, then incubated at 37 °C for 10 min to form hydrogels before adding warm E8 medium containing 10 μM ROCK inhibitor (Y-27632, Selleckchem). Medium was changed daily and cells were routinely passaged every 5 days. To passage cells, medium was removed, and 2 ml ice-cold PBS was added to dissolve the hydrogel for 5 min. Cell spheroids were collected by spinning at 100 g for 3 min. Cells were incubated in Accutase (Invitrogen) at 37 °C for 10 min and dissociated into single cells, and dissociated into single cells for re-encapsulation, as mentioned above. The NucleoCounter NC-200 (Chemometec) was used to count cell number.

2.3. hPSC spheroids differentiation and fusion experiment

hPSCs (~3000 cells) in 200 μl E8 medium was placed in one V-shape low attachment well of a 96-well plate for 48 h to form one hPSC spheroid. For cortical neuron differentiation, the hPSC spheroid was cultured in a cortical neuron induction medium containing 50% DMEM/F12 + 50% Neurobasal medium, 1% N2 (Life Technologies), 2% B27 (Life Technologies), SB431542 (10 μM, Selleckchem) and LDN193189 (100 nM, Selleckchem) for 11 days to differentiate hPSCs into cortical progenitor cells. Medium was changed daily. The progenitor cells were matured in a neural differentiation medium containing Neurobasal® Media (Life Technologies), BDNF (20 ng ml^{-1}, PeproTech), GDNF (10 ng ml^{-1}, PeproTech), L-ascorbic acid (200 μM, Sigma), Dibutyryl-cAMP (0.5 mM, Santa Cruz Biotechnology) and 2.5 μM DAPT (Selleckchem) for another 20 days. For ventral midbrain dopaminergic neuron differentiation, the hPSC spheroid was cultured in a ventral midbrain neuron induction medium containing 50% DMEM/F12 + 50% Neurobasal medium, 1% N2, 2% B27, SB431542 (10 μM), LDN193189 (100 nM), CHIR99021 (0.7 μM, Selleckchem), purmorphamine (2 μM, Selleckchem) and SHH (200 ng ml^{-1}, R&D Systems) for 11 days to differentiate hPSCs into DA progenitor cells. Medium was changed daily. The progenitor cells were matured in a neural differentiation medium containing Neurobasal® Media (Life Technologies), BDNF (20 ng ml^{-1}), GDNF (10 ng ml^{-1}), L-ascorbic acid (200 μM), Dibutyryl-cAMP (0.5 mM) and 2.5 μM DAPT for another 20 days. For the spheroid fusion experiments, on varied days along the differentiation, two spheroids were placed in one V-shape well of the 96-well plate. The fusion process was then imaged with microscopy.

2.4. Neural tissue biofabrication

Spheroids containing about 5–10 million hPSCs were harvested from the PNIPAAm-PEG hydrogel on day 5, suspended in E8 medium and placed in a 6.5 mm Polyester Membrane Transwell Insert (8 μm pore, Corning). Cells were then cultured in the cell culture incubator. For some samples, 5 h later, the medium was removed and a thin layer of ECM (5 μl) (Matrigel, BD Biosciences) was overlaid on top of the fused tissue. Medium was added back to culture the cells. To biofabricate the cortical neural tissue, the fused hPSC tissue was cultured in the cortical neuron induction medium for 11 days and matured in the neural differentiation medium for another 20 days. To biofabricate the ventral midbrain dopaminergic neural tissue, the fused hPSC tissue was cultured in the ventral midbrain neuron induction medium for 11 days and the neural differentiation medium for another 20 days.

2.5. Staining and imaging

To assess the pluripotency of hPSCs cultured in hydrogels, hPSC spheroids were harvested and dissociated into single cells with Accutase and stained in suspension. Cells were fixed with 4% paraformaldehyde (PFA) at room temperature for 15 min, permeabilized with 0.25% Triton X-100 for 10 min, and blocked with 5% goat serum for 1 h before incubating with primary antibodies at 4 °C overnight. After extensive washing, secondary antibodies and 10 μM 4′,6-Diamidino-2-Phenylindole (DAPI) in 2% BSA were added and incubated at room temperature for 4 h. Cells were washed 3 times with PBS before imaging with a fluorescence microscope. The percentage of Oct4+ or Nanog+ nuclei was quantified with Image J. Around 10 000 cells were analyzed.

To stain, the 3D tissues were fixed with 4% PFA at room temperature for 2 h, then incubated with PBS + 0.25% Triton X-100 + 5% goat serum + primary antibodies at 4 °C for 3 days. After extensive washing (3 × 8 h), secondary antibodies and 10 μM DAPI in 2% BSA was added and incubated at 4 °C for 1 day. Cells were washed with PBS for 3 times (8 h each) before imaging with confocal microscope. Antibodies used: Oct4 (1:200, Santa Cruz Biotech); Nanog (1:200, Santa Cruz Biotech); PAX6 (1:300, Covance); Otx2, Tuj1 (1:5000, Sigma); Tbr1, FOXA2 (1:200, Santa Cruz Biotech); Lmx1a (1:500, Millipore) and TH (1:500, PelFreez). The images were analyzed with Image J for quantification. Around 5000 cells were analyzed.

3. Results

We first confirmed that large numbers of uniform hPSC spheroids could be economically produced in

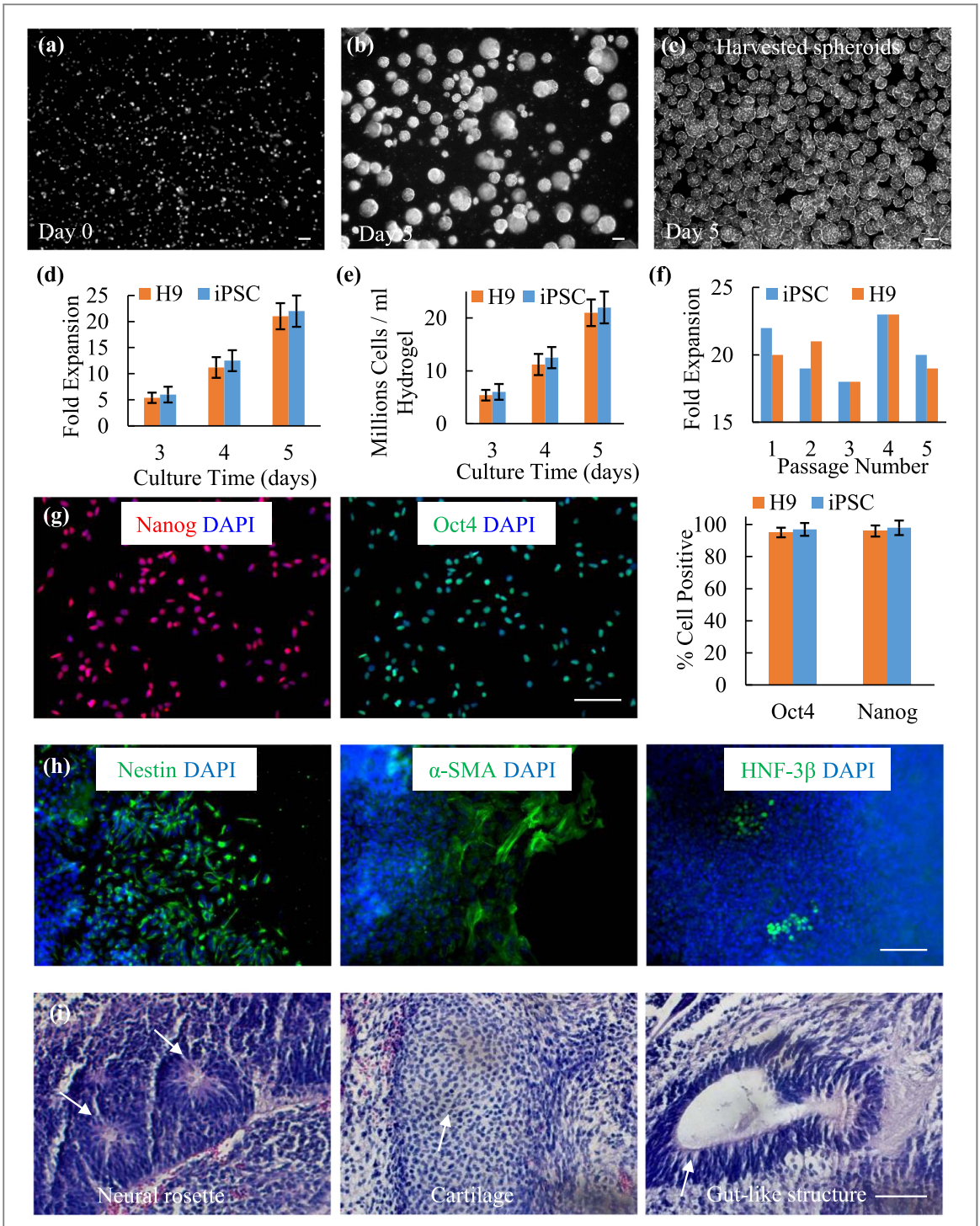

Figure 1. Biomanufacturing hPSC (H9 and iPSC) spheroids in thermoreversible PNIPAAm-PEG hydrogels. Single hPSCs were encapsulated in the PNIPAAm-PEG hydrogel and cultured in the Essential 8 (E8) medium. Single hPSCs (a) grew into uniform spheroids (b). On day 5, spheroids were harvested (c). Around 5-, 10- and 20-fold expansion was achieved, yielding ~5, 10 and 20 million cells per ml of hydrogel on day 3, 4 and 5, respectively ((d), and (e)). Consistent 20-fold expansion per 5 days was seen from passage 1 to 5 during the long-term hPSC culture within the hydrogel (f). After long-term culturing, above 95% cells were positive for the pluripotency markers, Oct4 and Nanog (g). (h) These hPSCs could be differentiated into the Nestin+ ectodermal, α-SMA+ mesodermal and HNF-3β+ endodermal cells in the *in vitro* embryoid body assay. (i) When transplanted to mice, they formed teratomas containing all the three germ layer tissues, such as the ectodermal neural rosette, the mesodermal cartilage and endodermal gut-like structure (arrows). Scale bars: 100 μm.

the thermoreversible PNIPAAm-PEG hydrogel [15]. We used both H9 hESCs and iPSCs to test the generality of the culture system. Single hPSCs grew into uniform spheroids on day 5 (figures 1(a)–(c)). hPSCs expanded around 5-, 10- and 20-fold on day 3, 4, and 5 of the culture, yielding around 5, 10, and 20×10^6 cells per ml of hydrogel, respectively (figures 1(d) and (e)). hPSC spheroids could be harvested by liquefying the hydrogel through cooling their temperature, i.e. adding ice-cold PBS for 5 min hPSCs could be cultured for multiple passages within the hydrogel with around 20-fold expansion every 5

days (figure 1(f)). After long-term culture, >95% of the cells remained pluripotency as shown by the expression of pluripotency markers, Nanog and Oct4 (figure 1(g)). Their pluripotency was further confirmed with the embryoid body assay *in vitro* and teratoma assay *in vivo*. hPSCs could be differentiated into Nestin+ ectodermal cells, α-SMA+ mesodermal cells and HNF-3β+ endodermal cells in the embryoid body assay (figure 1(h)). When transplanted to NOD-SCID mice, hPSCs formed teratomas containing all the three germ layer tissues, such as the ectodermal neural rosette, the mesodermal cartilage tissues and the endodermal gut-like structures (figure 1(i)). In summary, large numbers of hPSC spheroids could be readily made in the thermoreversible PNIPAAm-PEG hydrogels.

Based on the literature [44], we then developed protocols for differentiating hPSC spheroids into cortical neural tissue spheroids and ventral midbrain dopaminergic neural tissue spheroids. For cortical neural tissue differentiation, a cortical neuron induction medium containing small molecules LDN193189 and SB431542, which inhibit the dual SMAD signaling [44], was applied for 11 days to induce hPSCs into cortical progenitors. The spheroids were further cultured in a neural differentiating medium for an additional 20 days to mature the progenitor cells into neurons (figure 2(a)). On day 7, immunostaining showed ~90% cells in the spheroid were positive for the neural stem cell makers, PAX6 and Nestin (figures 2(b) and (d)). On day 30, ~80% cells in the spheroid were Tuj1 + neurons (figures 2(c) and (d)). For dopaminergic neural tissue differentiation, a neural induction medium containing small molecules LDN193189, SB431542, purmorphamine and CHIR99021, as well as protein SHH was applied to the hPSC spheroid for 11 days [24]. LDN193189 and SB431542 can induce hPSCs toward neural lineage, while SHH and purmorphamine can pattern cells to the ventral fate and CHIR99021 can pattern cells to the midbrain fate. Together, these molecules pattern hPSCs to the ventral midbrain dopaminergic neuron progenitor cells [24]. The spheroid was further cultured in the aforementioned neural differentiating medium for an additional 20 days to mature the progenitor cells into neurons (figure 2(e)). On day 11, ~90% cells in the spheroid were positive for the ventral midbrain progenitor makers, FOXA2 and Lmx1a (figures 2(f) and (h)). On day 30, ~80% cells in the spheroid were Tuj1 + and ~50% tyrosine hydroxylase positive (TH+) ventral midbrain dopaminergic neurons (figures 2(g) and (i)). No significant cell death was observed during the differentiation.

Quick and efficient spheroid fusion is crucial for the subsequent tissue maturation and thus is required for rapid tissue biofabrication, especially through bioprinting. We then quantitatively studied the fusion rate of undifferentiated and differentiated hPSC spheroids (figures 3 and 4). One hPSC spheroid was placed in a V-shape low attachment well of a 96-well plate and differentiated to a cortical neural tissue spheroid using aforementioned protocol (figure 2(a)). At different days along the differentiation, two spheroids were placed in one V-shape well to allow them to contact quickly. Their fusion process was then recorded with microscopy (figure 3(a)). We used the $(\pi r^2)/(\pi R^2)$, wherein r and R are the radius of the interface of the two spheroids and radius of the spheroid, respectively, to quantitatively measure the percentage of the spheroid fusion completed (figure 3(b)). And $t_{1/2}$ is referred to the time when 50% of the fusion is completed or $(\pi r^2)/(\pi R^2) = 0.5$ (figure 3(c)). We found that undifferentiated hPSC spheroids completed the fusion in 5 h. As the differentiation progressed, the fusion rates of spheroids decreased. The fusion became extremely slow after 14 days of differentiation. The $t_{1/2}$ of undifferentiated hPSC spheroids, spheroids differentiated for 4, 7, 14 and 28 days is 2.4, 2.6, 8.1, 66.6 and 90.6 h, respectively (figure 3(c)). Similar trends were found for ventral midbrain dopaminergic neural tissue spheroids (figure 4). The $t_{1/2}$ of undifferentiated hPSC spheroids, spheroids differentiated for 3, 6, 13 and 27 days is around 4.0, 6.0, 9.0, 11.0 and 16.0 h, respectively (figure 4(c)). Based on these results, we concluded that using neural tissue spheroids to biofabricate neural tissues would be limited by the slow fusion rate, and the Method 1 described in the introduction would be more appropriate for biofabricating tissues from hPSCs.

We then studied whether the fused hPSC tissue could be differentiated and matured into neural tissues. When spheroids were placed in a Transwell insert, they sedimented to the bottom and tightly packed within 10 min due to gravity (figures 5(a) and (b)) without centrifugation. Phase images showed packed individual spheroids at 10 min after placing them in the Transwell insert (figure 5(b), left). After 3 h, they fused to form a continuous tissue with rough surface (figure 5(b), middle). After 5 h, the surface became very smooth, indicating the completion of spheroids' fusion (figure 5(b), right). Live/dead cell staining showed very few dead cells within the fused hPSC tissue (figure 5(c)).

We then treated this hPSC tissue with the cortical neuron induction medium for 11 days and the neural differentiation medium for additional 20 days as described in figure 2(a). On day 5, small islands with diameters around 100 μm were frequently observed in the developing tissue (figure 6(a)). On day 11, a thin tissue that could not be lifted from the underlying Transwell insert was formed (figure 6(b)). Immunostaining showed ~75% of the cells in this thin tissue were positive for the cortical progenitor makers, PAX6 and Otx2 (figures 6(c) and (d)). On day 30, more than 80% cells were Tuj1+ neurons and 50% were positive for the cortical neuron marker, Tbr1 (figures 6(f) and (g)). However, we were unable to make a thick, 3D

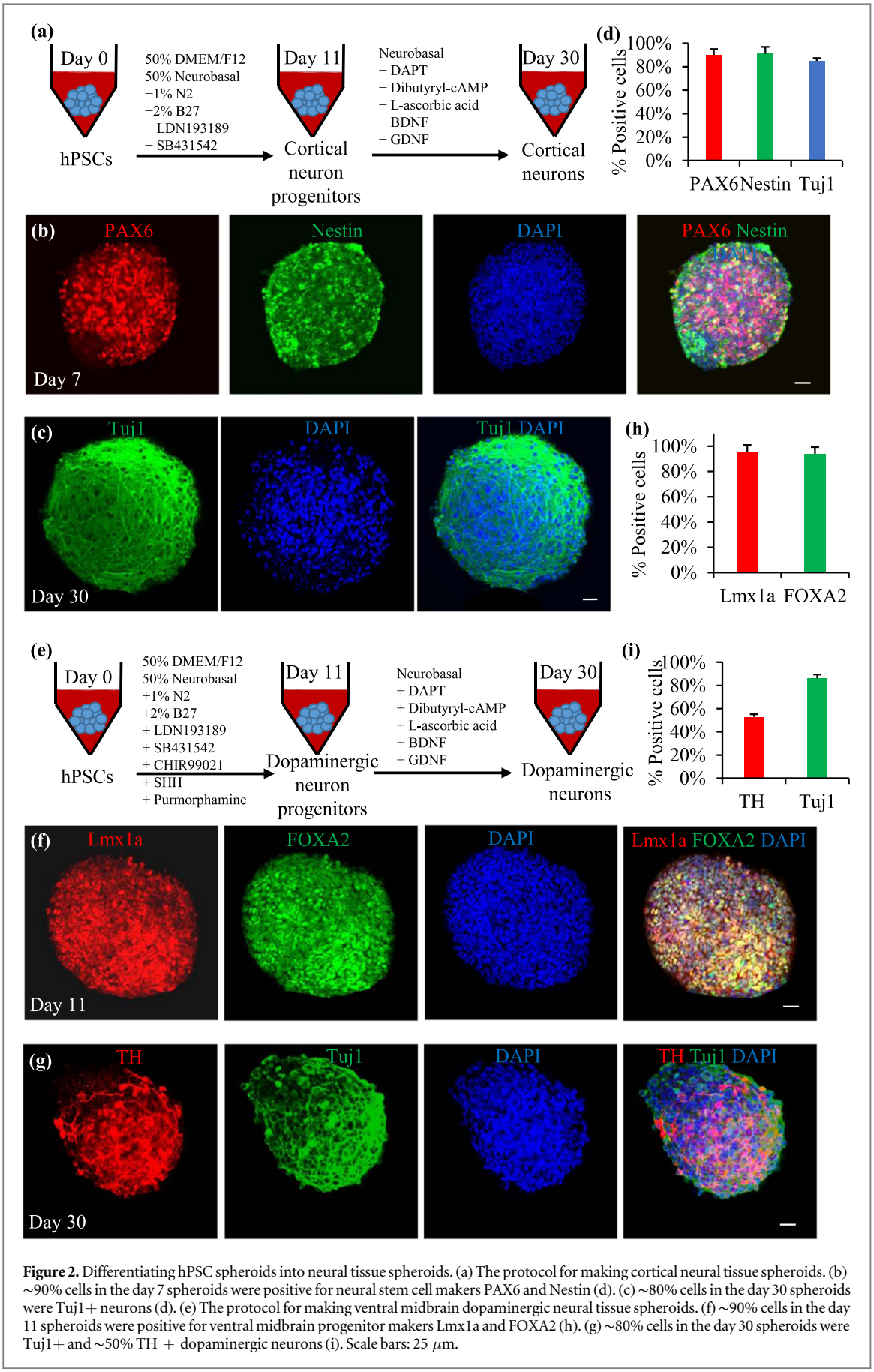

Figure 2. Differentiating hPSC spheroids into neural tissue spheroids. (a) The protocol for making cortical neural tissue spheroids. (b) ~90% cells in the day 7 spheroids were positive for neural stem cell makers PAX6 and Nestin (d). (c) ~80% cells in the day 30 spheroids were Tuj1+ neurons (d). (e) The protocol for making ventral midbrain dopaminergic neural tissue spheroids. (f) ~90% cells in the day 11 spheroids were positive for ventral midbrain progenitor makers Lmx1a and FOXA2 (h). (g) ~80% cells in the day 30 spheroids were Tuj1+ and ~50% TH + dopaminergic neurons (i). Scale bars: 25 μm.

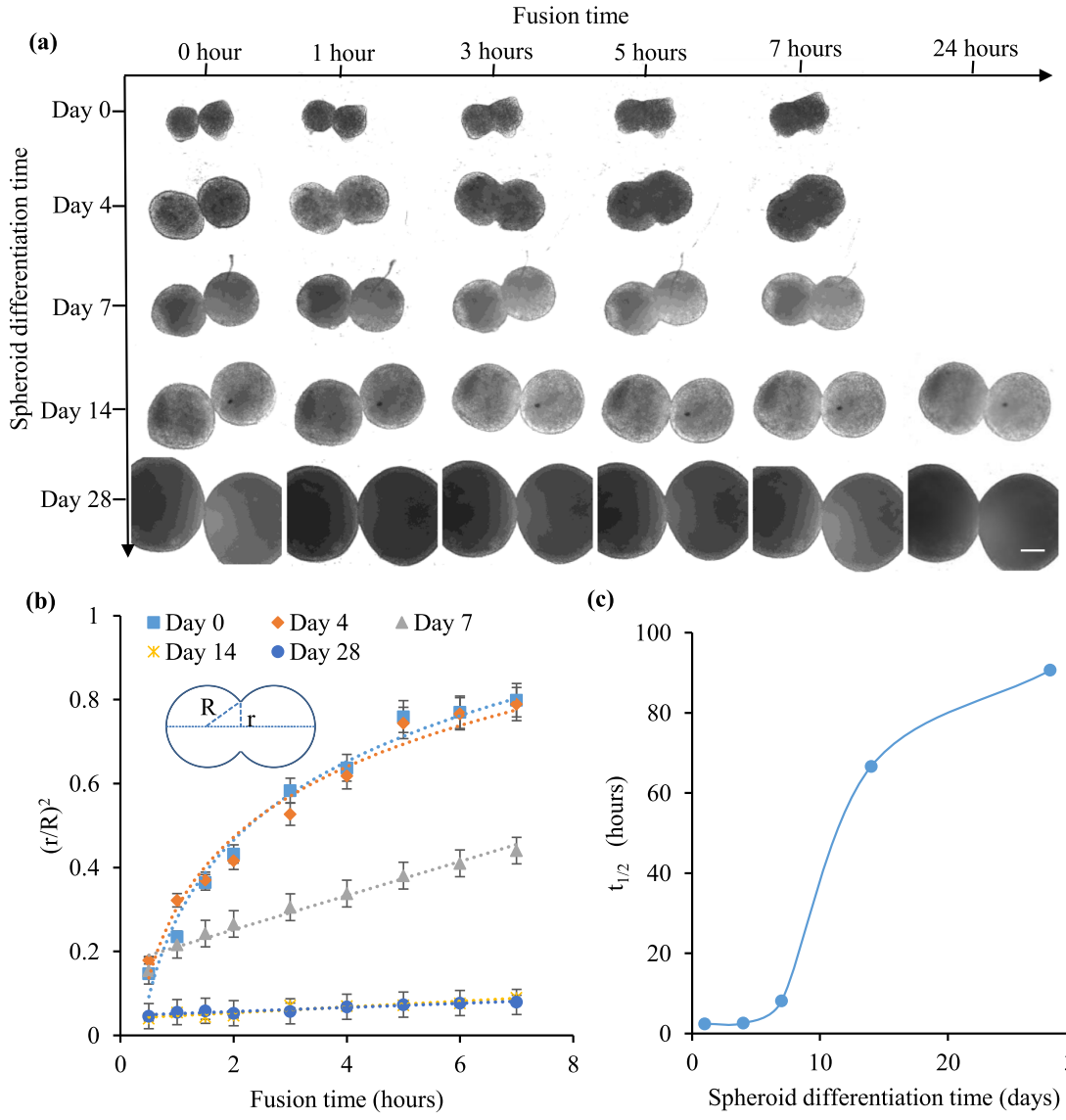

Figure 3. Spheroid fusion experiment. hPSC spheroids were differentiated toward cortical neural tissue spheroids, as described in figure 2(a). On day 0, 1, 4, 7, 14 and 28 along the differentiation, two spheroids were placed in contact and the fusion process was imaged at 0, 1, 3, 5, 7 and 24 h later. (a) Phase images of their fusion. (b) $(r/R)^2$ is used to measure their fusion rates. R and r is referred to the radius of a spheroid and the radius of the interface of the two fused spheroids, respectively. (c) $t_{1/2}$, the time to complete 50% fusion or $(r/R)^2 = ½$, is measured. Scale bars: 200 μm.

cortical tissue (figure 6(e)); instead, neurons clustered into aggregates (figure 6(f)).

We also treated the hPSC tissue with the ventral midbrain dopaminergic neuron induction medium for 11 days and the neural differentiation medium for additional 20 days as described in figure 2(e). Similar results were obtained. On day 5, cell islands were frequently seen in the developing tissue (figure 7(a)). On day 11, a thin tissue that could not be lifted from the underlying Transwell insert was formed (figure 7(b)). Immunostaining showed ~85% of the cells were positive for the ventral midbrain progenitor makers, FOXA2 and Lmx1a (figures 7(c) and (d)). On day 30, more than 90% cells were Tuj1+ neurons and 50% were positive for the ventral midbrain dopaminergic neuron marker, TH (figures 7(f) and (g)). Again, we were unable to make a 3D tissue (figure 7(e)); instead, neurons clustered into aggregates (figures 7(e) and (f)). In summary, although hPSCs could be differentiated into neurons, the fused hPSC tissues could not be converted into 3D neural tissues.

Literature studies showed that ECM were necessary for mammalian cells to assemble into 3D tissues [45]. We hypothesized that the loss of 3D structure during the hPSC tissue differentiation was due to the shortage of ECM. To test the hypothesis, a thin layer (~5 μm) of Matrigel was overlaid on the hPSC tissue prior to the neural induction. The hPSC tissue was then differentiated as aforementioned. Low concentration of Matrigel proteins (e.g. the commercial Matrigel product was diluted 100 fold) was supplemented to the culture medium during the 30 days. On day 5, no cell islands were observed (figure 8(a)), and on day 11, a soft, transparent and 3D tissue with

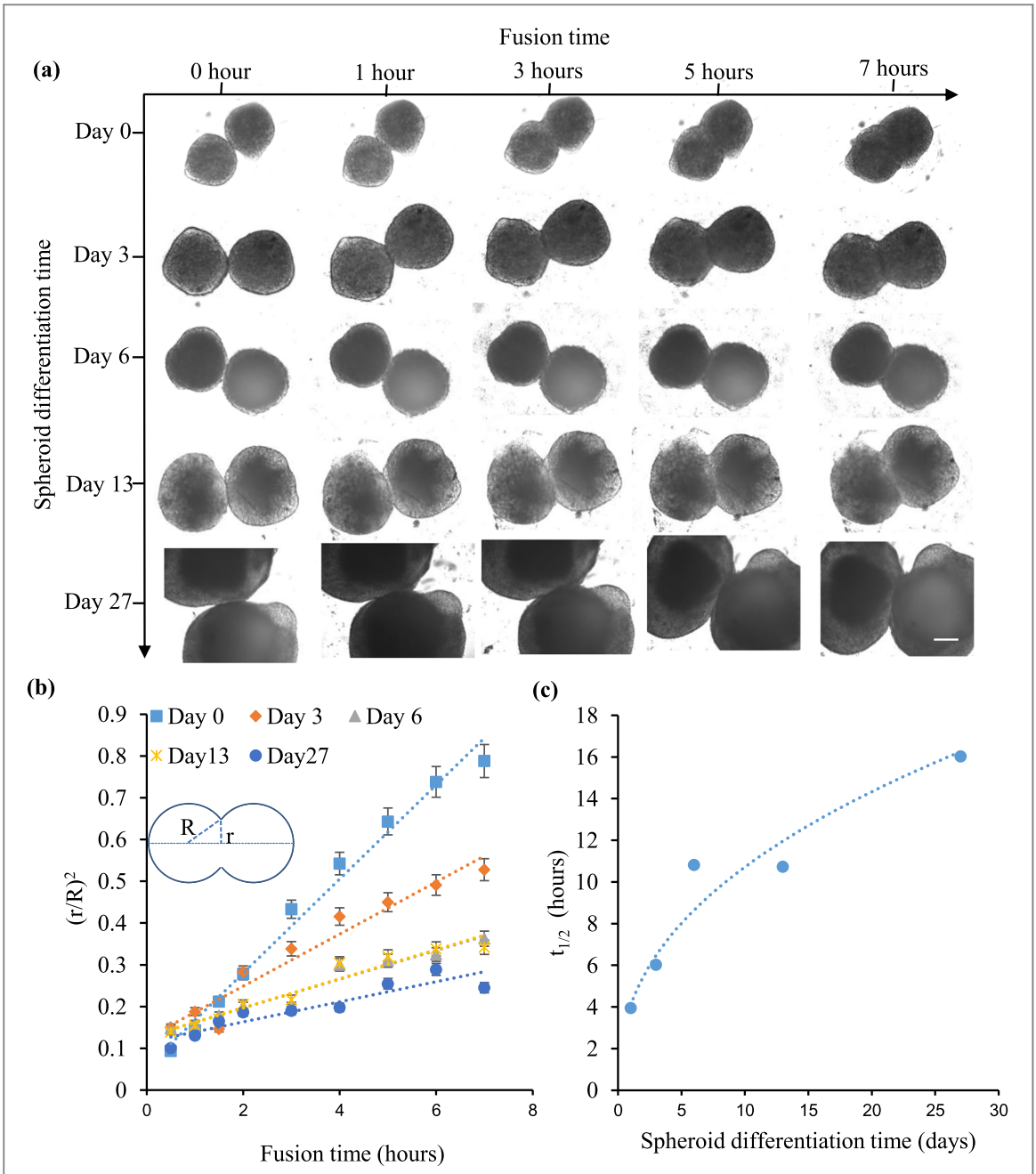

Figure 4. Spheroid fusion experiment. hPSC spheroids were differentiated toward ventral midbrain dopaminergic neural tissue spheroids, as described in figure 2(e). On day 0, 3, 6, 13 and 27 along the differentiation, two spheroids were placed in contact and the fusion process was imaged at 0, 1, 3, 5, 7 and 24 h later. (a) Phase images of their fusion. (b) $(r/R)^2$ is used to measure their fusion rates. R and r is referred to the radius of a spheroid and the radius of the interface of the two spheroids, respectively. (c) $t_{1/2}$, the time to complete 50% fusion or $(r/R)^2 = ½$, is measured. Scale bars: 200 μm.

thickness around 1 mm was formed (figures 8(b) and (c)). Immunostaining showed ~75% of the cells within the tissue were positive for the cortical progenitor cell markers, PAX6 and Otx2 (figures 8(d) and (e)). No Nanog+ or Oct4+ hPSCs were detected in the tissue (figure 8(f)). Further maturation in the neural differentiation medium, a 3D (~1 mm thickness), elastic and semi-transparent cortical tissue was produced (figures 8(g) and (h)). ~85% of the cells within the day 30 tissue were Tuj1+ neurons and ~50% were positive for the cortical neuron marker, Tbr1 (figures 8(i) and (j)).

Similar results were obtained when the hPSC tissue was overlaid with Matrigel and differentiated toward the dopaminergic neural tissue. On day 5, no cell islands were observed (figure 9(a)). On day 11, a soft, transparent and 3D tissue with thicknesses around 1 mm was formed (figures 9(b) and (c)). Immunostaining showed ~85% of the cells within the tissue were positive for the ventral midbrain progenitor makers, FOXA2 and Lmx1a (figures 9(d) and (e)). No Nanog+ or Oct4+ hPSCs were detected in the tissue (figure 9(f)). Further maturation in the neural differentiation medium, an elastic, semi-transparent

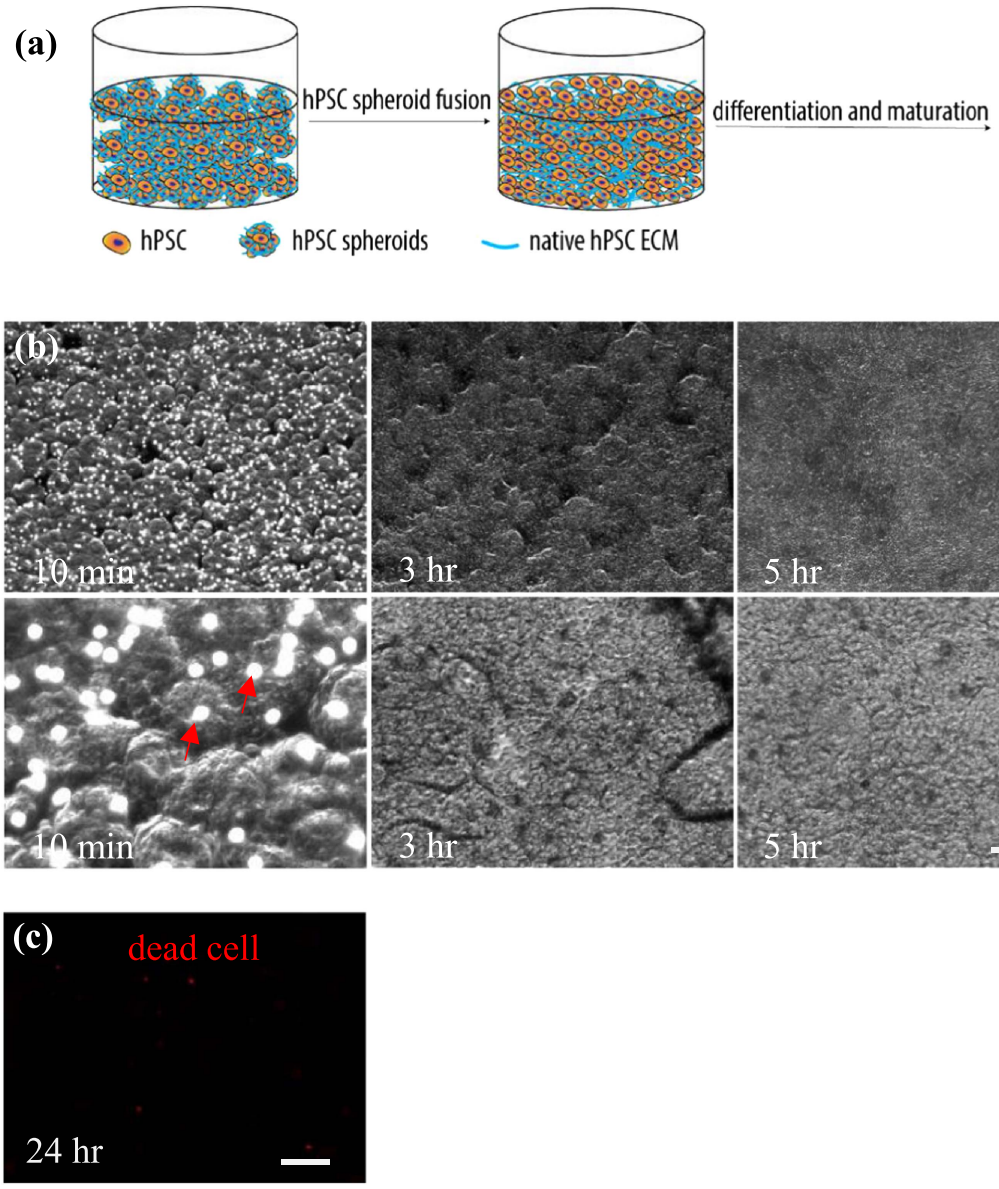

Figure 5. Biofabricating hPSC tissues. hPSC spheroids were harvested and placed in a Transwell insert to fuse into a cohesive tissue (a). Spheroids sedimented to the bottom of the insert within 10 min (b, left). The white dots (red arrows) were the pores of the insert. 3 h later, a continuous 3D tissue was formed (b, middle). 5 h later, the surface of the tissue became very smooth, indicating the completion of the fusion process (b, right). Top views of the samples were shown (b). Live/dead cell staining at 24 h showed very few dead cells within the tissue (c). Scale bars: 100 μm.

and 3D (~1 mm thickness) ventral midbrain tissue was produced (figures 9(g) and (h)). More than 90% cells were Tuj1+ neurons and 52% were positive for the ventral midbrain dopaminergic neuron marker, TH (figures 9(i) and (j)). In summary, hPSC tissues were successfully converted into 3D neural tissues in the presence of exogenous ECM.

4. Discussion

We biofabricate neural tissues including the cortical neural tissue and midbrain dopaminergic tissue to explore the tissue biofabrication methodology using hPSCs as starting materials in this study. Compared with neurons cultured in 2D, 3D neural tissues more closely resemble the *in vivo* brain tissues and thus are superior for investigating neurobiology and diseases, for drug discovery, and for treating neural diseases [46]. For instance, in the brains of Alzheimer's disease patients, large amounts of insoluble amyloid beta (Aβ) plaques are formed within the extracellular matrix. iPSCs derived from AD patients can be made and differentiated into brain neurons to model the disease *in vitro* [47]. However, the production of Aβ plaques in 2D cell culture is difficult due to the limited extracellular matrix in 2D cultures. A recent study showed that, in 3D neural tissues made from neural stem cells overexpressing three AD-causing genes, large amounts of Aβ plaques were made within their ECM [48]. Thus, 3D neural tissues made through the method developed in this study can be very valuable

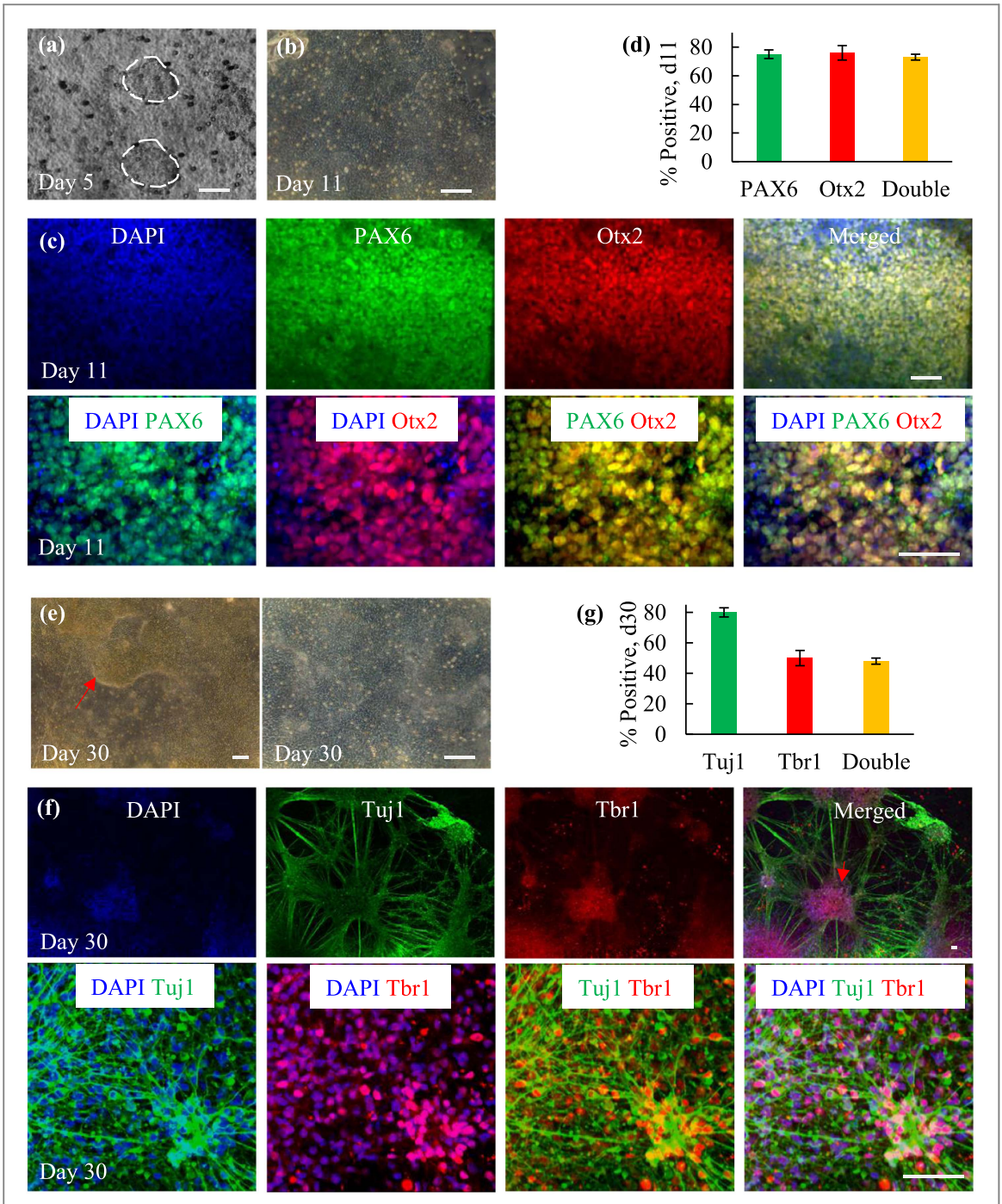

Figure 6. Biofabricating cortical neural tissues. The hPSC tissue was treated with neural induction and neural differentiation medium as described in figure 2(a). Cell islands (outlined with white dash lines) appeared on day 5 (a) during the differentiation. A thin cell sheet was formed on day 11 (b). The white dots seen in (b) were the pores of the insert. 75% of the cells were positive for the cortical neuron progenitor markers, PAX6 and Otx2 ((c) and (d)). On day 30, cells were differentiated into cortical neurons. 80% of the cells were Tuj1 + neurons and 50% were Tbr1+ cortical neurons ((f) and (g)). No 3D neural tissues were formed. Cells aggregated into clusters (red arrows) ((e) and (f)). ((a), (b) and (e)) Top views of the tissue. Scale bars: 50 μm.

for modeling brain diseases, particularly those with pathology in ECMs. In a second example, 3D neural tissues could be used to study glioblastoma, the most aggressive brain tumor. Glioblastoma cannot be completely removed through surgery because the tumor cells can infiltrate several centimeters into the surrounding brain tissues. The biofabricated 3D neural tissues can be used to study how tumor cells invade the brain tissue. In addition to studying the biology, these 3D neural tissues can be applied for discovering drugs that can prevent forming or dissolve Aβ plaques or stop the tumor cell invasion. Biofabricated 3D neural tissues can also be very useful for treating neural diseases and injuries. Transplanting of neural stem cells or neurons is being widely investigated for treating neural diseases and injuries. A current challenge with cell transplantation is the low survival of the transplanted cells *in vivo*. In general, about 5% to 10% of the cells can survive, limiting the efficacy of cell therapies [49]. Our laboratory research

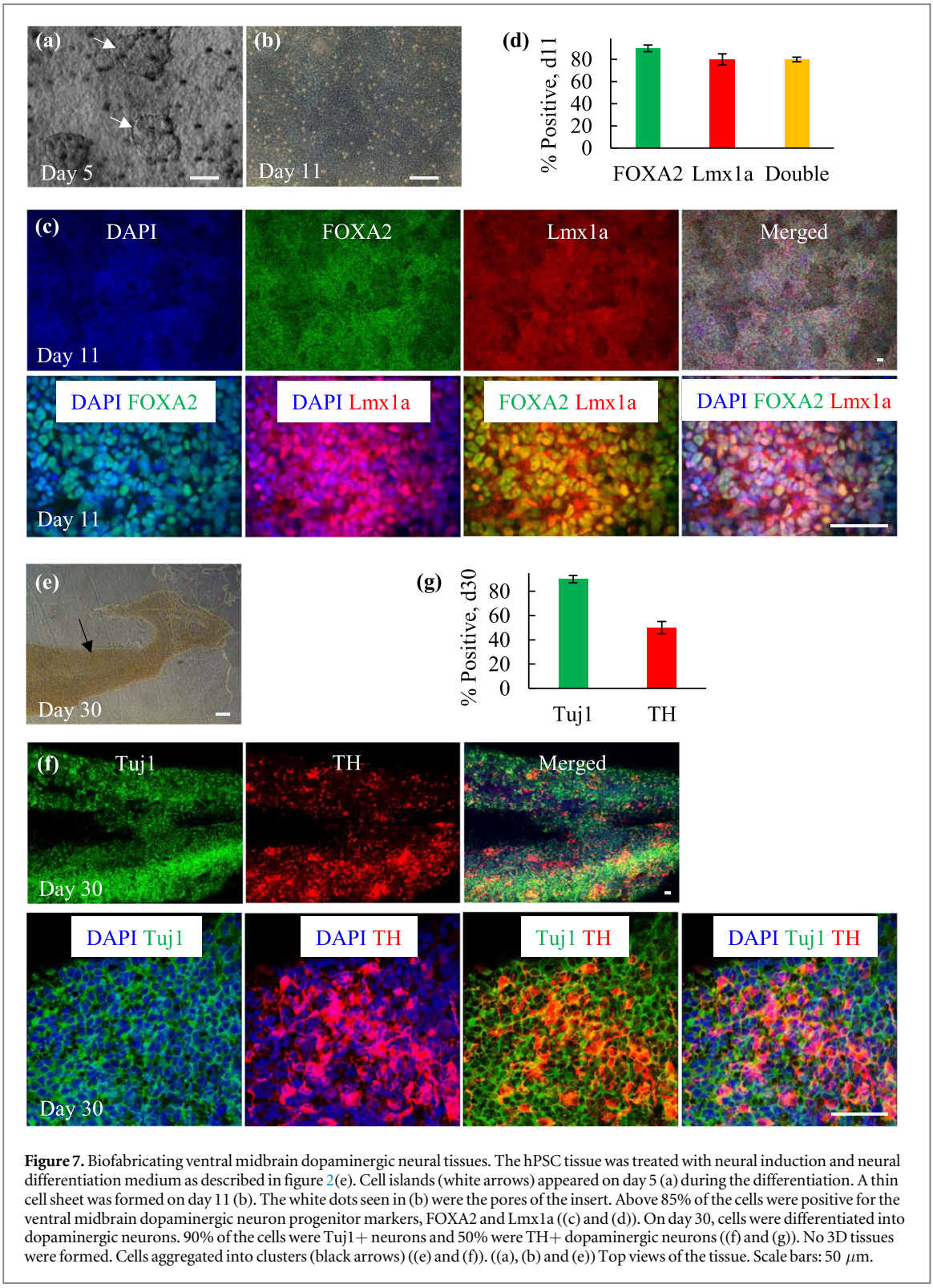

Figure 7. Biofabricating ventral midbrain dopaminergic neural tissues. The hPSC tissue was treated with neural induction and neural differentiation medium as described in figure 2(e). Cell islands (white arrows) appeared on day 5 (a) during the differentiation. A thin cell sheet was formed on day 11 (b). The white dots seen in (b) were the pores of the insert. Above 85% of the cells were positive for the ventral midbrain dopaminergic neuron progenitor markers, FOXA2 and Lmx1a ((c) and (d)). On day 30, cells were differentiated into dopaminergic neurons. 90% of the cells were Tuj1+ neurons and 50% were TH+ dopaminergic neurons ((f) and (g)). No 3D tissues were formed. Cells aggregated into clusters (black arrows) ((e) and (f)). ((a), (b) and (e)) Top views of the tissue. Scale bars: 50 μm.

as well as other research has shown that transplanting 3D neural tissues, rather than 2D cell cultures, could significantly improve cell survival and function *in vivo* [50]. Thus, biofabricated 3D tissues may be better than cells as cellular products for regenerative medicine.

As aforementioned, large numbers of hPSC spheroids are required for tissue biofabrication. To scale up the hPSC production, three-dimensional (3D) suspension culture systems, such as spinner flasks and stirred-tanks have been studied [40, 51]. Three components, cells; a medium; and stirring or shaking are within these systems. Ideally, the seeded single hPSCs initially associate to form small clusters that subsequently expand to generate uniform spheroids. In reality, these spheroids frequently aggregate during the culture to form large agglomerates, resulting in two negative consequences [52]. First, the produced spheroids varied significantly in their size and

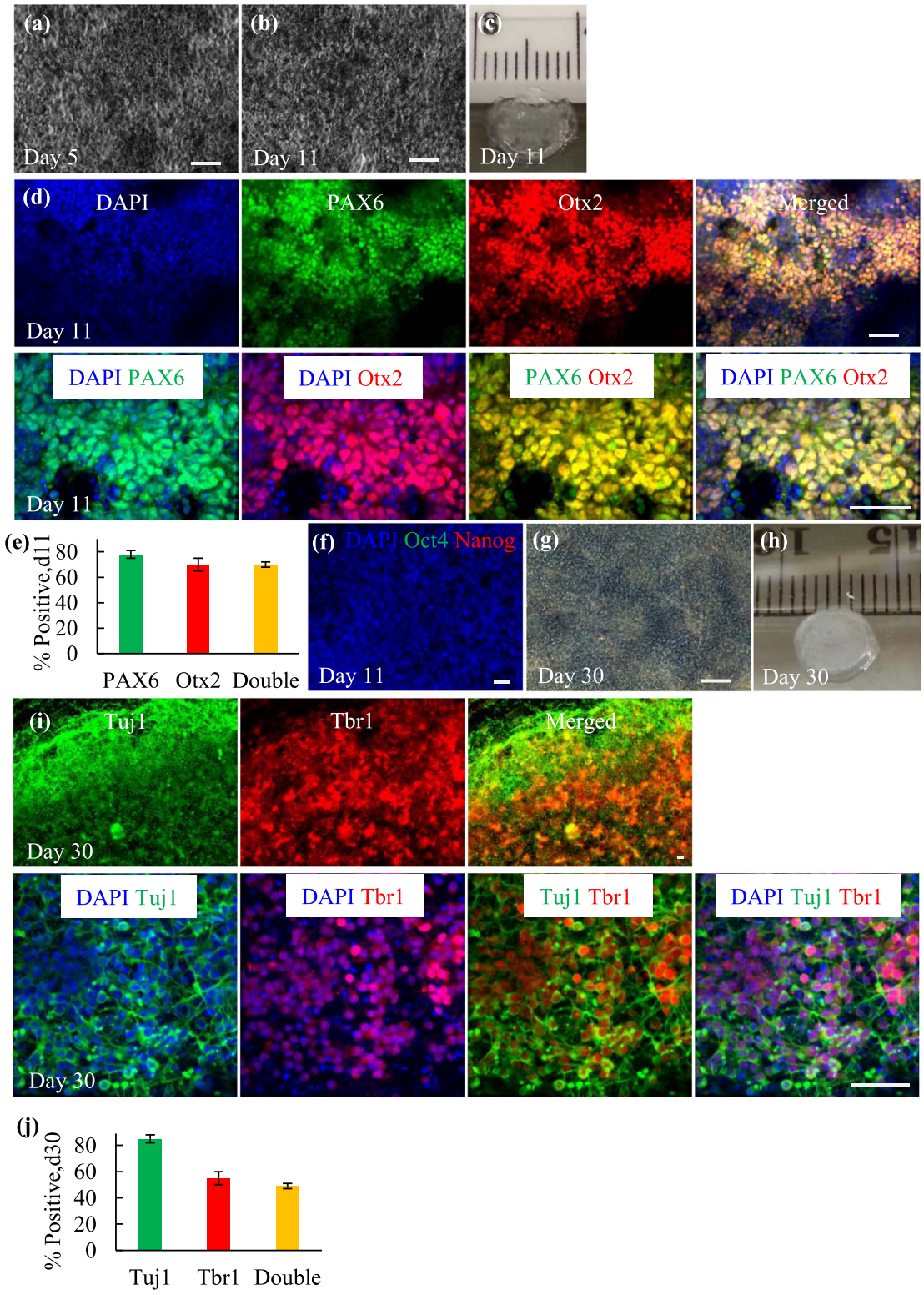

Figure 8. Biofabricating cortical neural tissues in the presence of exogenous ECM. The hPSC tissue was overlaid with a thin layer of Matrigel and treated with neural induction and neural differentiation medium as described in figure 2(a). Cell islands were not seen on day 5 (a) during the differentiation. A 3D, soft and transparent tissue was formed on day 11 ((b) and (c)). 75% of the cells were positive for the cortical neuron progenitor markers, PAX6 and Otx2 ((d) and (e)). No Nanog+ or Oct4+ hPSCs were found in the tissue (f). A 3D, elastic and semi-transparent cortical tissue was formed on day 30 ((g) and (h)). 85% of the cells were Tuj1+ neurons and 55% were Tbr1+ cortical neurons ((i) and (j)). ((a), (b) and (g)) Top views of the tissue. Scale bars: 50 μm.

characteristics. Second, it is well known that the transport of nutrients, oxygen and growth factors, and the metabolic waste from cells located at the center of agglomerates with diameters >500 μm become insufficient, leading to slow cell proliferation, apoptosis, and uncontrolled differentiation [53]. While stirring or shaking reduces spheroid agglomeration, they also generate hydrodynamic stress that negatively

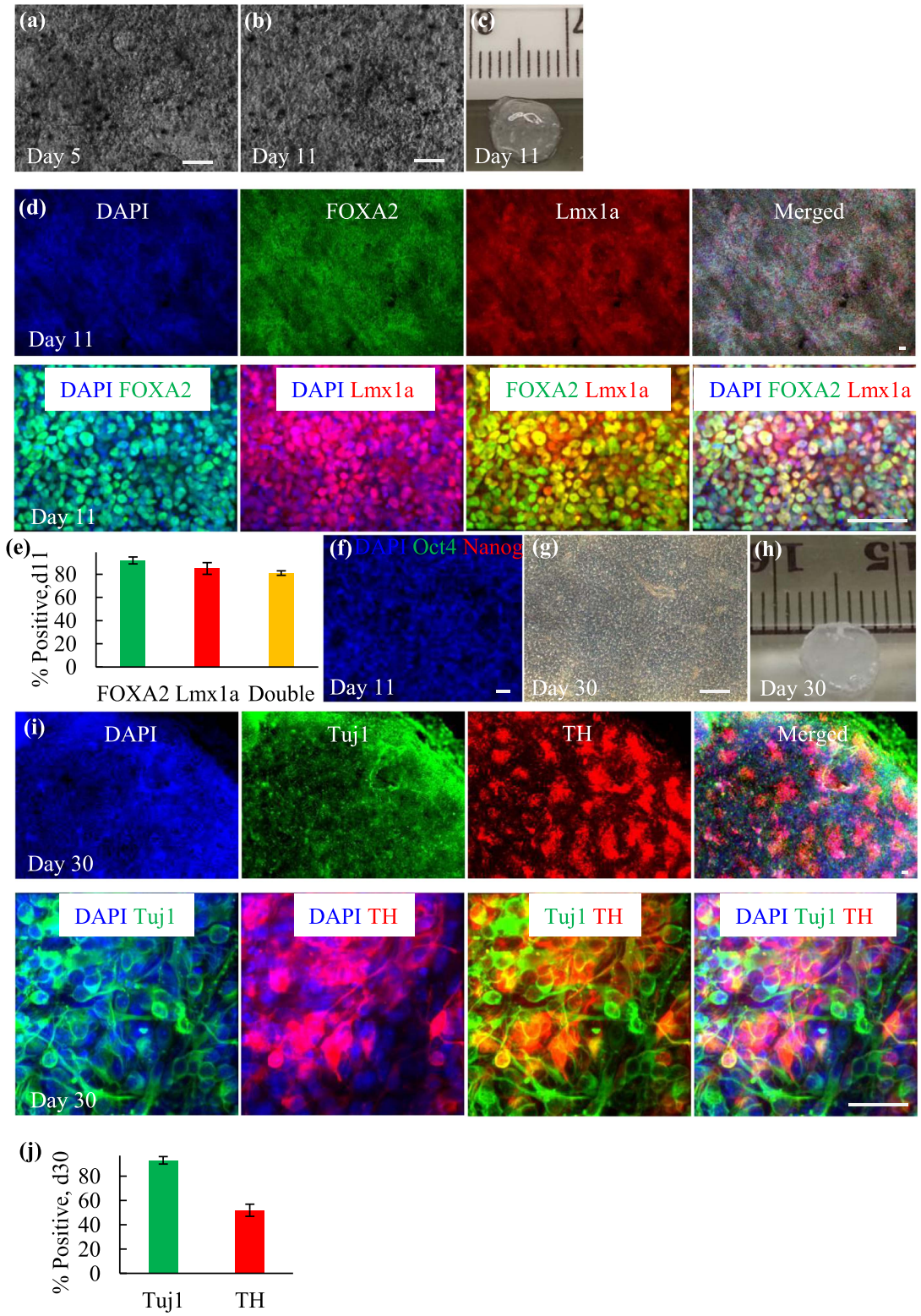

Figure 9. Biofabricating ventral midbrain dopaminergic tissues in the presence of exogenous ECM. The hPSC tissue was overlaid with a thin layer of Matrigel and treated with neural induction and neural differentiation medium as described in figure 2(e). Cell islands were not seen on day 5 (a) during the differentiation. A 3D, soft and transparent tissue was formed on day 11 ((b) and (c)). Above 85% of the cells were positive for the ventral midbrain dopaminergic neuron progenitor markers, FOXA2 and Lmx1a ((d) and (e)). No Nanog+ or Oct4+ hPSCs were found in the tissue (f). A 3D, elastic and semi-transparent ventral midbrain tissue was formed on day 30 ((g) and (h)). 93% of the cells were Tuj1+ neurons and 52% were TH+ dopaminergic neurons ((i) and (j)). ((a), (b) and (g)) Top views of the tissue. Scale bars: 50 μm.

affects cell growth [54, 55]. High cell density in the culture also promotes spheroid agglomeration [14]. Considering all these factors, in current suspension culture studies, hPSCs are generally seeded at low density (e.g., ~3 $\times$ 10^5 cells/mL) and stirred at 70 to 120 rotations-per-minute (rpm). Under even these

optimized conditions, slow cell growth, significant cell death, phenotype change, genomic mutations, and low volumetric yield are common [40]. For instance, we and others showed iPSCs typically expanded 4-fold per 4 days to yield around 2.0×10^6 cells/mL in suspension cultures [14, 15, 40]. It is good to note that cells occupy <0.2% of the medium or bioreactor volume with this yield. This low yield results in extremely high biomanufacturing cost. This challenge can be answered with the PNIPAAm-PEG hydrogel culture system (figure 1). The hydrogel scaffold not only provides space for cell growth, but also acts as physical barriers to prevent the neighboring spheroids from agglomeration and isolate the hydrodynamic stress. These lead to high cell viability, proliferation and yield, as well as uniform spheroid size. For instance, 20-fold expansion per 5 days to yield 2.0×10^7 cells has been achieved.

An essential requirement for rapid tissue biofabrication is that spheroids can quickly fuse to form a cohesive tissue. Culturing hPSCs in 3D thermoreversible PNIPAAm-PEG hydrogels allowed the production of spheroids which contained both cells and their native ECM (figure 1) [56]. Spheroids placed in contact with one another quickly fused into 3D tissues. The driven force for tissue fusion is the minimization of the tissue surface free energy [57, 58]. Through tissue fusion, cells can maximize their interactions with neighboring cells and ECM. hPSC spheroids harvested from hydrogel sedimented, packed and fused within 3 h (figures 5(a) and (b)). No cell death was observed during the fusion (figure 5(c)). Notably, when hPSCs from 2D cultures or dissociated spheroids (e.g. single cells) were placed in contact, a minimal of 24 h were required for cells to fuse into a cohesive tissue and large percentage of cells went apoptosis (data not shown), indicting the importance of the native ECM for the spheroid fusion and highlighting the advantage of using the PNIPAAm-PEG hydrogels for culturing hPSCs.

An important finding of this study is that the fusion rate decreased significantly once hPSC spheroids were differentiated (figures 3 and 4). This is particularly obvious for the cortical neural tissue spheroids (figure 3). This phenomenon leads us to conclude that a more appropriate method to biofabricate neural tissues is to fuse hPSC spheroids first, followed by differentiating and maturing the hPSC tissue. Importantly, our study also showed that the hPSCs in the hPSC tissue could be differentiated into neurons with protocols similar to these used for differentiating hPSCs into neurons in 2D culture (figure 2). It should be noted that not all the hPSCs in the biofabricated tissues were differentiated into the desired neurons in this study. These biofabricated tissues are appropriate for modeling diseases and drug discovery. For *in vivo* application, the differentiation protocols should be optimized to quantitatively convert hPSCs into the desired neurons in the future.

The finding that extra ECM were needed to form 3D neural tissues during the differentiation of hPSC tissues can be explained by the inability of neurons to produce enough ECM (figures 6 to 9). *In vivo*, the ECM in the brain are produced by glia cells [59]. In the biofabricated tissues, there are no or little glia cells to produce ECM. Matrigel was supplemented as exogenous ECM to facilitate the 3D tissue formation in this research. Matrigel, a solubilized basement membrane preparation extracted from the mouse sarcoma, however, is animal-derived, not defined, and not qualified for biomanufacturing cells for clinical applications [60]. Future research to replace Matrigel is necessary in order to biomanufacture 3D tissues for clinical application. Notably, adding exogenous ECMs did not significantly change the differentiation process and efficiency. The cellular compositions in the day 11 and day 30 tissues produced without or with exogenous ECM were very similar (figure 6 versus 7 and figure 8 versus 9).

Biofabricating tissues through first fusing hPSC spheroids, followed by differentiation and maturation is simple, however, this also has limitations. First, the biofabricated tissues lack vasculature. A solution to this challenge is to use bio-printer to print a sacrificing hydrogel network in the hPSC tissue [61]. After the hPSC tissue becomes the mature neural tissue, the sacrificing hydrogel network is removed and endothelial and smooth muscle cells are seeded to the channels to form the vasculature. Both the PNIPAAm-PEG and alginate hydrogels can be used for this purpose. They can be removed by cooling the temperature or adding EDTA for a few minutes. The second challenge is to biofabricate neural tissues with multiple types of neurons. This challenge can be solved by using the progenitor tissue spheroids as building blocks to biofabricate the cohesive tissue. For instance, the day 11 cortical progenitor and the day 11 ventral midbrain progenitor tissue spheroids can be bio-printed into a cohesive tissue that can be further matured into a neural tissue with two types of neurons. Our study showed the progenitor spheroids could fuse, through their fusion rates were slower than hPSC spheroids (figures 3 and 4).

5. Conclusion

In summary, this study explored some fundamentals and methods for biofabricating tissues using hPSCs as the cell source. We found: (1) the PNIPAAm-PEG hydrogel culture system was excellent for biomanufacturing hPSC spheroids; (2) the spheroid fusion experiment was a quick and efficient method to evaluate the fusion capability of tissue spheroids; (3) the fusion rates of differentiated spheroids were significantly lower than hPSC spheroids; (4) hPSCs could be differentiated into tissue cells in the 3D tissues; and (5) the method by first fusing hPSC spheroids, followed

with differentiation and maturation was appropriate for tissue biofabrication.

Acknowledgments

This work was partially funded by Nebraska DHHS Stem Cell Research Project (to Y.L.). Confocal microscope imaging was done in the Morrison Microscopy Core Research Facility at University of Nebraska, Lincoln. Drs. You Zhou and Christian Elowsky assisted the confocal imaging.

Author Contributions

YL, HL and QL conceived the idea and designed the study. HL and QL performed experiments and analyzed data. YL wrote the manuscript.

Competing financial interests

The authors declare no competing financial interests.

References

[1] Wobma H and Vunjak-Novakovic G 2016 Tissue engineering and regenerative medicine 2015: a year in review *Tissue Eng. Part B Rev.* **22** 101–13

[2] Langer R and Vacanti J P 1993 Tissue engineering *Science* **260** 920–6

[3] Page C O F, Griffith L G and Naughton G 2002 Tissue engineering-current challenges and expanding opportunities *Science* **295** 1009–14

[4] Mironov V, Boland T, Trusk T, Forgacs G and Markwald R R 2003 Organ printing: computer-aided jet-based 3D tissue engineering *Trends Biotechnol.* **21** 157–61

[5] Mironov V, Visconti R P, Kasyanov V, Forgacs G, Drake C J and Markwald R R 2009 Organ printing: tissue spheroids as building blocks *Biomaterials* **30** 2164–74

[6] Mironov V, Kasyanov V and Markwald R R 2011 Organ printing: from bioprinter to organ biofabrication line *Curr. Opin. Biotechnol.* **22** 667–73

[7] Novosel E C, Kleinhans C and Kluger P J 2011 Vascularization is the key challenge in tissue engineering *Adv. Drug. Deliv. Rev.* **63** 300–11

[8] Mason C 2006 The time has come to engineer tissues and not just tissue engineer *Regen. Med.* **1** 303–6

[9] Khademhosseini A, Langer R, Borenstein J and Vacanti J P 2006 Microscale technologies for tissue engineering and biology *Proc. Natl Acad. Sci. USA* **103** 2480–7

[10] Lokmic Z and Mitchell G M 2008 Engineering the microcirculation *Tissue Eng. Part B Rev.* **14** 87–103

[11] Langer R 2007 Editorial: tissue engineering: perspectives, challenges, and future directions *Tissue Eng.* **13** 1–2

[12] Laschke M W and Menger M D 2016 Life is 3D: boosting spheroid function for tissue engineering *Trends Biotechnol.* **35** 133–44

[13] Olsen T R and Alexis F 2014 Bioprocessing of tissues using cellular spheroids *Bioprocess. Biotech.* **4** 1000e112

[14] Lei Y, Jeong D, Xiao J and Schaffer D V 2014 Developing defined and scalable 3D culture systems for culturing human pluripotent stem cells at high densities *Cell. Mol. Bioeng.* **7** 172–83

[15] Lei Y and Schaffer D V 2013 A fully defined and scalable 3D culture system for human pluripotent stem cell expansion and differentiation *Proc. Natl Acad. Sci. USA* **110** E5039–48

[16] Thomson *et al* 1998 Embryonic stem cell lines derived from human blastocysts *Science* **282** 1145–7

[17] Takahashi K, Tanabe K, Ohnuki M, Narita M, Ichisaka T, Tomoda K and Yamanaka S 2007 Induction of pluripotent stem cells from adult human fibroblasts by defined factors *Cell* **131** 861–72

[18] Chen G *et al* 2011 Chemically defined conditions for human iPSC derivation and culture *Nat. Methods* **8** 424–9

[19] Shi Y, Kirwan P, Smith J, Robinson H P C and Livesey F J 2012 Human cerebral cortex development from pluripotent stem cells to functional excitatory synapses *Nat. Publ. Gr.* **15** 477–86

[20] Shi Y, Kirwan P and Livesey F J 2012 Directed differentiation of human pluripotent stem cells to cerebral cortex neurons and neural networks *Nat. Protoc.* **7** 1836–46

[21] Liu Y, Liu H, Sauvey C, Yao L, Zarnowska E D and Zhang S-C 2013 Directed differentiation of forebrain GABA interneurons from human pluripotent stem cells *Nat. Protoc.* **8** 1670–9

[22] Maroof A M *et al* 2013 Directed differentiation and functional maturation of cortical interneurons from human embryonic stem cells *Cell Stem Cell* **12** 559–72

[23] Hunt R F, Girskis K M, Rubenstein J L, Alvarez-Buylla A and Baraban S C 2013 GABA progenitors grafted into the adult epileptic brain control seizures and abnormal behavior *Nat. Neurosci.* **16** 692–7

[24] Kriks S *et al* 2011 Dopamine neurons derived from human ES cells efficiently engraft in animal models of Parkinson's disease *Nature* **480** 547–51

[25] Kirkeby A, Grealish S, Wolf D A, Nelander J, Wood J, Lundblad M, Lindvall O and Parmar M 2012 Generation of regionally specified neural progenitors and functional neurons from human embryonic stem cells under defined conditions *Cell Rep.* **1** 703–14

[26] Orlova V V, van den Hil F E, Petrus-Reurer S, Drabsch Y, Ten Dijke P and Mummery C L 2014 Generation, expansion and functional analysis of endothelial cells and pericytes derived from human pluripotent stem cells *Nat. Protoc.* **9** 1514–31

[27] Prasain N *et al* 2014 Differentiation of human pluripotent stem cells to cells similar to cord-blood endothelial colony-forming cells *Nat. Biotechnol.* **32** 1151–7

[28] Lian X, Bao X, Al-Ahmad A, Liu J, Wu Y, Dong W, Dunn K K, Shusta E V and Palecek S P 2014 Efficient differentiation of human pluripotent stem cells to endothelial progenitors via small-molecule activation of WNT signaling *Stem Cell Reports* **3** 804–16

[29] Kimbrel E A *et al* 2014 Mesenchymal stem cell population derived from human pluripotent stem cells displays potent immunomodulatory and therapeutic properties *Stem. Cells Dev.* **23** 1611–24

[30] Nishio M and Saeki K 2014 Differentiation of human pluripotent stem cells into highly functional classical brown adipocytes *Methods Enzymol.* **537** 177–97

[31] Burridge P W *et al* 2014 Chemically defined generation of human cardiomyocytes *Nat. Methods* **11** 855–60

[32] Lian X, Hsiao C, Wilson G, Zhu K, Hazeltine L B, Azarin S M, Raval K K, Zhang J, Kamp T J and Palecek S P 2012 Robust cardiomyocyte differentiation from human pluripotent stem cells via temporal modulation of canonical Wnt signaling *Proc. Natl Acad. Sci. USA* **109** E1848–57

[33] Lian X, Zhang J, Azarin S M, Zhu K, Hazeltine L B, Bao X, Hsiao C, Kamp T J and Palecek S P 2013 Directed cardiomyocyte differentiation from human pluripotent stem cells by modulating Wnt/β-catenin signaling under fully defined conditions *Nat. Protoc.* **8** 162–75

[34] Si-Tayeb K, Noto F K, Nagaoka M, Li J, Battle M A, Duris C, North P E, Dalton S and Duncan S A 2010 Highly efficient generation of human hepatocyte-like cells from induced pluripotent stem cells *Hepatology* **51** 297–305

[35] Hannan N R F, Segeritz C-P, Touboul T and Vallier L 2013 Production of hepatocyte-like cells from human pluripotent stem cells *Nat. Protoc.* **8** 430–7

[36] Szkolnicka D, Farnworth S L, Lucendo-Villarin B and Hay D C 2014 Deriving functional hepatocytes from pluripotent stem cells *Curr. Protoc. Stem Cell Biol.* **30** 1–1G

[37] Rezania A *et al* 2014 Reversal of diabetes with insulin-producing cells derived *in vitro* from human pluripotent stem cells *Nat. Biotechnol.* **32** 1121–34

[38] Pagliuca F W, Millman J R, Gu M, Segel M, Dervort A V, Ryu J H, Peterson Q P, Greiner D and Melton D A 2014

Resource generation of functional human pancreatic β cells *in vitro* *Cell* **159** 428–39
[39] Polak J M and Mantalaris S 2008 Stem cells bioprocessing: an important milestone to move regenerative medicine research into the clinical arena *Pediatr Res* **63** 461–6
[40] Serra M, Brito C, Correia C and Alves P M 2012 Process engineering of human pluripotent stem cells for clinical application *Trends Biotechnol.* **30** 350–8
[41] Lin H, Li Q and Lei Y 2017 An integrated miniature bioprocessing for personalized human induced pluripotent stem cell expansion and differentiation into neural stem cells *Sci. Rep.* **7** 40191
[42] Li Q, Lin H, Wang O, Qiu X, Kidambi S and Lei Y 2016 Scalable production of glioblastoma tumor-initiating cells in 3 dimension thermoreversible hydrogels *Sci. Rep.* **6** 31915
[43] Park I H, Zhao R, West J A, Yabuuchi A, Huo H, Ince T A, Lerou P H, Lensch M W and Daley G Q 2008 Reprogramming of human somatic cells to pluripotency with defined factors *Nature* **451** 141–6
[44] Chambers S M, Fasano C A, Papapetrou E P, Tomishima M, Sadelain M and Studer L 2009 Highly efficient neural conversion of human ES and iPS cells by dual inhibition of SMAD signaling *Nat. Biotechnol.* **27** 275–80
[45] Sasai Y, Eiraku M, Suga H and Glossary B 2012 *In vitro* organogenesis in three dimensions: self-organising stem cells *Development* **4121** 4111–21
[46] Ravi M, Paramesh V, Kaviya S R, Anuradha E and Solomon F D 2014 3D cell culture systems—advantages and applications *J. Cell. Physiol.* **230** 16–26
[47] Kondo T *et al* 2013 Modeling Alzheimer's disease with iPSCs reveals stress phenotypes associated with intracellular Aβ and differential drug responsiveness *Cell Stem Cell* **12** 487–96
[48] Choi S H *et al* 2014 A three-dimensional human neural cell culture model of Alzheimer's disease *Nature* **515** 274–8
[49] Brundin P, Karlsson J, Emgård M, Schierle G S, Hansson O and Petersén A C R 2000 Improving the survival of grafted dopaminergic neurons: a review over current approaches *Cell Transpl.* **9** 179–95
[50] Clarkson E D, Zawada W M, Adams F S, Bell K P and Freed C R 1998 Strands of embryonic mesencephalic tissue show greater dopamine neuron survival and better behavioral improvement than cell suspensions after transplantation in parkinsonian rats *Brain Res.* **806** 60–8
[51] Gouzheng W, Zhang W, Rich M and Gossain V 2009 Growing CHO cells in a CelliGen ® BLU benchtop, stirred-tank bioreactor using single-use vessels *Biotechnol. Prog.* **1** 1–4 (http://www.biotechniques.com/multimedia/archive/00074/New_Brunswick-FP-Cel_74610a.pdf)
[52] Hajdu Z, Mironov V, Mehesz A N, Norris R A, Markwald R R and Visconti R P 2010 Tissue spheroid fusion-based *in vitro* screening assays for analysis of tissue maturation *J. Tissue Eng. Regen. Med.* **4** 659–64
[53] Grimes D R, Kannan P, McIntyre A, Kavanagh A, Siddiky A, Wigfield S, Harris A and Partridge M 2016 The role of oxygen in avascular tumor growth *PLoS One* **11** e0153692
[54] Hu W, Berdugo C and Chalmers J J 2011 The potential of hydrodynamic damage to animal cells of industrial relevance: current understanding *Cytotechnology* **63** 445–60
[55] Brindley D, Moorthy K, Lee J-H, Mason C, Kim H-W and Wall I 2011 Bioprocess forces and their impact on cell behavior: implications for bone regeneration therapy *J. Tissue Eng.* **2011** 620247
[56] Ngangan A V and McDevitt T C 2009 Acellularization of embryoid bodies via physical disruption methods *Biomaterials* **30** 1143–9
[57] Ray H J and Niswander L 2012 Mechanisms of tissue fusion during development *Development* **139** 1701–11
[58] Fleming P A, Argraves W S, Gentile C, Neagu A, Forgacs G and Drake C J 2010 Fusion of uniluminal vascular spheroids: a model for assembly of blood vessels *Dev. Dyn.* **239** 398–406
[59] Wiese S, Karus M and Faissner A 2012 Astrocytes as a source for extracellular matrix molecules and cytokines *Front. Pharmacol.* **3** 1–13
[60] Kleinman H K and Martin G R 2005 Matrigel: basement membrane matrix with biological activity *Semin. Cancer Biol.* **15** 378–86
[61] Kang H, Lee S J, Ko I K, Kengla C, Yoo J J and Atala A 2016 A 3D bioprinting system to produce human-scale tissue constructs with structural integrity *Nat. Biotechnol.* **34** 312–9